American Journal of Innovation in Science and Engineering (AJISE)

ISSN: 2158-7205 (ONLINE)

VOLUME 4 ISSUE 1 (2025)

PUBLISHED BY
E-PALLI PUBLISHERS, DELAWARE, USA

American Journal of Innovation in Science and Engineering (AJISE)

Volume 4 Issue 1, Year 2025
ISSN: 2158-7205 (Online)
DOI: https://doi.org/10.54536/ajise.v4i1.3948
https://journals.e-palli.com/home/index.php/ajise

Compatibility Study of Synthesized Materials for Thermal Transport in Thermoelectric Power Generation

Christian Idogho[1*], Emmanuel Owoicho Abah[2], John Ejila Abel[3], Catur Harsito[4], Modupe Omoniyi[5], Temitope Boriwaye[1]

Article Information

Received: October 19, 2024
Accepted: November 29, 2024
Published: February 03, 2025

Keywords

Compatibility, Power Generation, Synthesized Materials, Thermoelectric, Thermal Transport

ABSTRACT

This study investigates the compatibility of synthesized materials for optimized thermal transport within thermoelectric modules. Experimental procedures involved the synthesis of candidate materials followed by characterization using techniques such as scanning electron microscopy, and thermal conductivity measurements. The research employs electrodeposition of $HoSb_xTe_x$ on the synthesized materials using AAo as a template in the electrolyte composed of 2mm TeO_2, 2.5mm $Bi(No_3)_3$, 0.33mm SeO_2, and 0.2m HNO_3. Compatibility assessments were conducted within simulated thermoelectric modules to evaluate the materials' performance under realistic operating conditions. The findings reveal crucial insights into the interplay between material properties and thermal transport mechanisms, guiding the selection and optimization of materials for enhanced thermoelectric power generation. Moreover, this study underscores the importance of tailored material design to achieve synergistic enhancements in both thermal and electrical conductivity, thereby advancing the efficiency and viability of thermoelectric energy conversion technologies. This research contributes to the ongoing efforts to enhance thermoelectric power generation and supports the global transition to sustainable energy systems.

INTRODUCTION

The world's ever-increasing population translates to a corresponding increase in the demand for energy to satisfy human consumption and industrial usage. For this, traditional non-renewable energy sources (fossil fuels) have become increasingly exhausted in a bid to quench the insatiable thirst for energy (Wang *et al.*, 2012). Currently, there is ongoing research to exploit cleaner sources of energy as regards efficiency and sustainability, and this research is nothing short of being highly desirable (Harsito *et al.*, 2022a; Karthick *et al.*, 2019). Among these emerging technologies, thermoelectric (TE) energy conversion has garnered widespread attention as it provides a captivating opportunity for the reliable, reversible, and direct energy conversion between heat and electricity thereby crucial to the areas of waste heat recovery, radioisotope power generation and refrigeration (Ali *et al.*, 2018; Pramudi *et al.*, 2024). The solid-state nature of the thermoelectric technique, its high reliability, and its long operating life, are chief among the advantages it provides. It also requires no mechanical moving parts thereby making it relatively scalable and noise-free (Lee *et al.*, 2020; Zhang *et al.*, 2018). Solid-state TE devices employ the Seebeck and Peltier effects in their operation. The former enables the transformation of thermal energy to electrical energy, and the latter conversely changes electric power to heat (Harsito *et al.* n.d; Thimont & LeBlanc, 2019). The fundamental idea under which thermoelectric power generation operates is simple. A temperature gradient is created across a heat source and a heat sink. Heat flows from the source to the sink through a thermoelectric converter (usually pairs of different semiconductor materials) that creates a voltage difference when exposed to the temperature gradient. This phenomenon is called the Seebeck effect. Uniquely, the configuration can be reversed to create a heat gradient from an electric current. This phenomenon is called the Peltier effect.

Materials play a key role in the overall output of every technological process and in fact, the transformation to renewable energy technologies should first of all be a materials transition. Hence, it is imperative to synthesize compounds and evaluate their compatibility for thermal transport in TEPGs, in such a way as to improve the efficiency of the TE materials for better results of the thermoelectric power generation. The efficiency of these TE materials is measured by a dimensionless figure of merit defined by $ZT = (\alpha^2/\rho k)T$, where α is the Seebeck coefficient, ϱ is the electric resistivity, k is the thermal conductivity and T is the absolute temperature. Therefore, an ideal and compatible TEPG material should possess a ZT value close to or greater than unity. A higher ZT value translates to better TE efficiency. Similarly, the material should have a large Seebeck coefficient to generate a large voltage, as the Seebeck coefficient reflects the ability of a material to generate a potential difference in response to a temperature change. It is equally important that the material possesses a low electrical resistivity for easy transport of charge carriers thereby minimizing

[1] Department of Material Science and Engineering, University of Vermont, Burlington, 05405, USA
[2] The Food Systems Research Center FSRC & Department of Extension, University of Vermont, USA
[3] Department of Mechanical Engineering, University of Agriculture Makurdi, 2373, Nigeria
[4] Mechanical Engineering Department, Vocational School of Universitas Sebelas Maret, Surakarta, 57126, Indonesia
[5] Department of Chemistry, University of Vermont, Burlington, 05405, USA
[*] Corresponding author's e-mail: christian.idogho@uvm.edu

joule heating and maximizing power output, and a low thermal conductivity to reduce heat dissipation and maintain a large temperature gradient across the material (Wang *et al.*, 2020). Hence, the research of heat transport characteristics in the framework of TEPG is critical to optimizing the design, stability, and performance of TE materials and devices in such a way as to lead to more effective and efficient thermoelectric power generation. Other key criteria to evaluate the compatibility of synthetic materials for thermal transport in TEPG include high thermal stability of the material across the operating temperature range to ensure its reliability and boost long-term performance. TE materials should also possess good mechanical properties such as high strength and flexural stability to boost the durability of TE generators in applications that induce mechanical stresses. The most common methods to assess the compatibility of synthetic materials with TEPG systems include the measurement of the thermoelectric properties (Seebeck coefficient, electrical conductivity, and thermal conductivity), calculating the figure of merit (ZT), mechanical testing (for thermal cycling stability, flexibility and durability), as well as the structural and compositional analysis of the materials (using techniques as scanning electron microscopy, x-ray diffraction, etc.) among several others.

Recently, the development and modification of thermoelectric power generators have opened doors to new materials for thermal transport in TEPG through the synthesis of conventional and non-conventional materials (Olivares-Robles *et al.*, 2020). Synthetic materials provide several benefits over conventional materials in thermoelectric applications such as the ability to optimize their transport properties for improved thermoelectric performance. Synthetic materials can also be tailored to provide better mechanical properties (strength, durability, flexibility, etc.) as well as to perform more efficiently across a broader range of temperatures. These enable them to be suitable for a wider range of TE applications and conditions. Furthermore, synthetic materials are more compatible and can be designed to integrate seamlessly with modern electronic technologies.

Over time, researchers have synthesized TEPG materials through several methods like alloying, doping, vapor-liquid-solid growth process, spark plasma sintering (SPS), physical vapor deposition (PVD), chemical vapor deposition (CVD), hydrothermal process, molecular beam epitaxy (MBE), electrodeposition, etc. While PVD and CVD are the most widely employed forms of deposition to synthesize TEPG materials, many researchers have preferred to use the electrodeposition technique adopted in this study, as it is comparatively more effective for creating nanostructured materials and composites. Electrodeposition is a method of choice to synthesize nanoengineered thermoelectric materials because of its low operating and capital costs, high deposition rates, easy scalability, near room temperature operation thus reducing problems with thermal stress, and the ability to tailor the properties of materials by adjusting deposition conditions (Xiao *et al.*, 2008).

This paper presents a new approach to assess the compatibility of HoSbxTex synthesized materials for thermal transport in TEPGs, considering the interplay between electrical conductivity, Seebeck coefficient, and thermal conductivity. Various pre-treatment processes such as ball milling and degassing, as well as careful consideration and choice of synthesis parameters and deposition methods, were carried out to ensure high purity, uniformity, and optimal thermoelectric properties of the synthesized materials. Also, post-annealing of the synthesized materials was carried out to reduce defect density and further improve material properties. A major stride in the current understanding of thermoelectric materials compatibility and performance was achieved, as the precise control over synthesis parameters and methods led to a significant reduction in the thermal conductivities of the synthesized materials with no negative impact on their high electrical conductivities, thus enhancing the resultant peak ZT values up to a range of 1.5 – 1.6.

In this paper, the criteria for TE materials selection are first discussed, followed by an overview of synthesized materials like Bismuth Telluride, skutterudites, and half-heuslers for thermoelectric applications. Next, the potential of emerging synthesized materials to offer better performance compared to traditional materials was discussed. The study continues with the overview of techniques such as scanning electron microscopy, and nanostructuring to enhance material compatibility and performance. Furthermore, it presents the simulation of some selected synthesized materials after the experimental synthesis and electrodeposition process to develop them. Finally, areas for further exploration are highlighted, including improving the compatibility and performance of TEPG materials by optimizing material synthesis, leg geometry, and operational parameters.

LITERATURE REVIEW

Over the years, there has been numerous and varying research on thermoelectric power generation, chiefly to continuously develop new materials with a significant increase in ZT values to enhance thermal transport and develop more efficient and scalable TEGs (Zhang *et al.*, 2018). The main problem in the TEG commercialization process is that the figure of merit (ZT) value of the material is still small (Maduabuchi & Gurevich, 2021). ZT~1 value is required in thermoelectric materials. The ZT value is highly dependent on temperature and varies with slight temperature changes. TEPG prototypes have been made with several materials with ZT values below 1, so the efficiencies of the TEPG devices are still far below 10%. Several types of new materials have been studied extensively, showing progress in ZT values and creating great opportunities in the development of STe_3 bulk materials with an average ZT~1.4 between 300 and 450K (Shittu *et al.*, 2020). Cu-doped BiTeSe materials maintained average ZT values slightly higher than unity (Wu *et al.*, 2018). The $AgPbMSbTe_2^+$ material has a maximum ZT

value of 2.2 at 800K (Ferreira-Teixeira & Pereira, 2018). Skutterudities have a ZT value of 1.7 at 850K (Ma *et al.*, 2019) and Silicon Germanium alloys ($Si_{80}Ge_{20}$) with ZT~1.84 at 1073K (Ferreira-Teixeira & Pereira, 2018). The increasingly diverse range of thermoelectric materials has given rise to the idea of combining two materials into one, so it is necessary to know the compatibility factors so that the materials can interact well and not harm each other (Harsito *et al.*, 2022a; Qui & Shi, 2020). When selecting materials and studying their compatibility for thermoelectric generation, several other factors need to be considered during operation as the thermoelectric generator experiences a large temperature gradient across it (Zhu *et al.*, 2020).

Twaha *et al.* reviewed the significance of reduced lattice thermal conductivity in improving the TE efficiency and ZT values of TE materials, in addition to allowing re-optimization of the carrier concentration, leading to more ZT improvement. They highlighted Zn_4Sb_3 as one of the most efficient TE materials owing to its extraordinarily low thermal conductivity and electronic structure of a heavily doped semiconductor, with a high ZT value between 450 and 670 K (ZT =1.3 at 670 K).

He *et al.* discussed the role of design optimization in developing high-performance TE devices. They stated that the design of TE devices requires a holistic approach of not just considering the ZT of thermoelectric materials, but also satisfactory contacts, thermal interfaces, mechanical properties, interconnects, and packaging techniques. In addition, they opined that half-Heusler compounds and nanocrystalline silicon could provide a combination of sought-after materials properties and that addressing the issues of reliability and lifetime of TE devices is equally as important as the design of TE devices. For example, long-term operation and thermal cycling of TEGs induce strong thermomechanical stress at the interface between the semiconductor and metal. Therefore, efforts should be aimed at greatly limiting these stresses to avoid critical failure of TE devices.

Maduabuchi & Mgbemene presented the introduction of nanostructures into films as an effective choice to obtain more efficient and compatible micro-TE devices as more cooling and electric output power could be obtained, compared to that of common films. However, in the drive to develop more efficient and compatible synthetic materials for thermal transport in TEPGs, researchers have utilized a host of techniques to achieve the desired results.

Wu *et al.* reviewed the latest development of various synthesized thermoelectric materials (i.e., Te, PbTe, Bi_2Te_3 and their derivatives, BiSe, BiS, Sb_2Te_3) in different forms including thin films, nanowires, and nanocomposites. They highlighted the indirect correlation between synthesized parameters and TE properties, as the material properties (e.g., morphology, composition, crystallinity, crystal structure) had direct effects on the TE properties. Hence, synthesized materials are utilized in fabricating TE devices, attributed to their ability to facilitate more efficient thermal transport of holes and electrons under controlled morphology, chemical composition, and crystal structure of the selected materials.

Morgan *et al.* investigated the suitability and potential of using physical vapor deposition (PVD) techniques with the roll-to-roll (R2R) process for high-throughput manufacturing of flexible TEGs. They demonstrated sputtering as a viable, scalable, and R2R-compatible technique for producing a flexible TEG. To verify PVD/R2R compatibility for thermoelectric applications, they investigated the thermoelectric properties of R2R sputtered Bi_2Te_3, and highlighted that higher power factors (PFs) and low electrical resistivities could be tuned by reducing deposition times, demonstrating PVD/R2R's potential as a high-speed, low-cost commercial system for flexible electronics. They also verified the novel high-deposition rate of the virtual cathode deposition (VCD), a special type of PVD technique. Results showed that VCD offers deposition speeds of more than 1 μm/min whilst maintaining substrate temperatures below 60 °C, making it fully compatible with a large array of low-temperature flexible substrates, and has the potential to be the future of high-throughput flexible electronic manufacturing for the wearable market via the R2R process.

Yoo *et al.* electrochemically deposited BixTey thin films grown from nitric acid baths on sputtered Au/Ni/Si substrates at room temperature with a fixed magnetic agitation rate of 300 rpm and a scan rate of 1 mV/s. Prior to potentiostatic deposition, linear sweep voltammograms (LSVs) were utilized to investigate the effect of Bi ion concentration. The study revealed that the film compositions and morphology were strongly dependent on the deposition conditions. Surface morphologies varied from granular to needle-like structures depending on the Te content of the films, while the power factor improved with the increase of Bi ions in the electrolytes.

Pallavi *et al.* also electrodeposited nanocrystalline Bismuth Telluride (Bi_2Te_3) thin films potentiostatically from an acidic bath at room temperature and an applied potential -0.4V versus saturated calomel electrode (SCE). The study indicated an increase in electrical conductivity of Bi_2Te_3 with an increase in temperature, as well as a negative value of Seebeck coefficient to show that Bi_2Te_3 is a n-type semiconductor.

Overall, research on synthesized TE materials has proved crucial in spurring advancement in various applications including TE devices, microelectronics, and thermal management systems, as novel materials with tailored properties, have been continually developed to meet the demands of the evolving modern technology.

Objective of Study

To fill the research gaps in the literature review, the current work dwells on the relative importance of the compatibility study of synthesized materials, in identifying optimal material combinations to enhance electrical conductivity and the Seebeck coefficient against the reduction in thermal conductivity, hence improving

the thermoelectric figure of merit (ZT) while maintaining other essential thermal transport properties within TEPGs.

MATERIALS AND METHODS

Experimental Synthesis of TEPG Materials for Thermal Transport

In studying the compatibility of synthetic materials for heat transport, thermoelectric materials (usually compounds) made up of two or more chemically combined elements are employed. For this study, $HoSb_xTe_x$ (x = 1.5 or x = 1.6) has been selected to verify its compatibility with other selected materials for heat transport from the hot side to the cold side in TEPG. The selected chemical compound is a member of the semiconductor thermoelectric power-generating materials. The semiconductor materials selected, have complex crystalline and electronic shapes for temperature distribution from the hot side to the cold side. Selecting the chemical compound composition may alter the structure and increase the properties of thermoelectric materials.

The following pre-treatment steps were carried out on the Ho, Sb, and Te powders [with 99.999% purity and supplied by Sigma-Aldrich (Merck)] before the actual synthesis. The individual components were precisely weighed according to the desired stoichiometry and then mixed thoroughly to achieve a uniform distribution of elements. The mixed powder was subjected to ball milling (in a controlled atmosphere to prevent oxidation) to break down agglomerates, reduce particle size, and ensure a homogeneous mixture. The mixture was then degassed under a vacuum to remove absorbed gases and moisture, thereby preventing unwanted reactions during the subsequent heating process. The mixture was finally cold-pressed into pellets to improve its density and uniformity and to facilitate better sintering during the heating process.

The following steps were employed in the actual synthesis of each specimen. Distilled water was added to the mixture of Ho, Sb, and Te powders to some ratios and heated for 168 hours (The prolonged heating duration was to ensure complete reaction and homogenization of the constituent elements. This helps to achieve a uniform composition and phase purity that is critical for the thermoelectric properties of Ho, Sb, and Te. The prolonged heating also allows sufficient time for atomic diffusion necessary for forming a well-ordered crystalline structure and eliminating defects), at a temperature of 750°C (This temperature was chosen based on the phase diagram and previous studies that indicate it as optimal for forming the Ho, Sb, Te phase. It is high enough to promote the reaction between Ho, Sb, and Te but below the melting point of the compound, ensuring a solid-state reaction without melting. This temperature also supports the growth of large, well-formed crystals that are beneficial in improving the materials' thermoelectric properties). The heated mixture was then evacuated in a crucible nitride covered with sealed fused silica ampoule, introduced into cold water, and quenched rapidly with chemical reactions in an argon atmosphere (The rapid quenching cools the material, preventing the formation of unwanted secondary phase and preserving the high-temperature phase structure. This helps in locking in the desired crystalline structure and preventing decomposition or phase transformation during cooling. Using argon helps to prevent oxidation and contamination during the cooling process. This is crucial as the presence of oxygen could lead to the formation of oxides which can deteriorate the thermoelectric properties of the compound). The crucible was then opened to enable the powdered mixture to react together, before being ground into agate mortar. The agate mixture was annealed through heating, cooled, and allowed to form a high-density specimen under a cylindrical press for some time with an accurate pressure of 76kpa and an atmospheric temperature of 873°C.

$HoSb_xTe_x$ was deposited on the selected materials (Bi_2SbTe_3, Bi_2Te_3, Zn_2Sb_3, $CeFe_4Sb_{12}$, Te/Ag/Ge/Sb, $Ce_{0.5}Fe_{3.5}Co_{0.5}Sb_{12}$, $Mo_3Sb_4Te_{1.6}$, and SiGe) one after the other through electrodeposition, using AAo as template in the electrolyte composed of 2mm TeO_2, 2.5mm $Bi(No_3)_3$, 0.33mm SeO_2, and 0.2m HNO_3. The post-annealing process was carried out at 300°C under an argon atmosphere. The electrodeposition of the synthetic materials combined potential controlled deposition pulses with galvanostatic controlled resting pulses. The synthetic materials deposited had uniform stoichiometric compositions along the entire thickness of 750µm at deposition rates of 50µm/h. The chemical composition of $HoSb_xTe_x$ can be controlled by varying Ho ion concentration in the electrolyte with 6mm $HTeO_2$+ and 2m HNO_3. The pulsed electrodeposition method was used to reduce the electrical resistivity of the films.

Linseis system (Model: LSR-3; Manufacturer: Linseis Messgeräte GmbH; Contact Material: Platinum) was used to measure the Seebeck coefficient, electrical conductivity, thermal conductivity, and electrical resistivity of the synthesized materials (Sample size: 5mm in diameter and 20mm in height) within maximum operating temperature range of 1500°C to -100°C. The measured values were then set as input engineering data for simulation using ANSYS Workbench.

Detecting Morphologies and Chemical Composition of the Synthesized Materials

Zeiss Sigma 300vp Field-Emission scanning electron microscope (SEM) was employed for this process, due to its ability to resolve objects in the micro or nano-metre range. It was operated at an accelerating voltage of 20KV, and the energy dispersive spectroscopy (EDS) equipped in SEM, was used to investigate the surface morphologies, chemical composition, and compatibility of the electrodeposited $HoSb_xTe_x$ with the synthesized materials.

X-ray diffraction (XRD) was used to confirm the crystal structure and reveal important information on the chemical composition of the synthesized materials, with patterns measured at 30KV and 30MA.

Principles for Measuring Material Parameters

Rectangular samples of the synthetic materials were vertically positioned between the Linseis (LSR-3) block lower electrode (which contains the heating coil or secondary heater) and the block upper electrode (for inverting the temperature gradient). Then, the entire arrangement was placed in a location furnace, which heats the sample to a certain temperature difference for measurement. When this temperature is reached, the heating coil in the lower electrode generates a pre-defined temperature difference along the sample. The temperatures of the two contacting thermocouples, T_1 and T_2 are used to measure the temperature difference ($\Delta T = T_2 - T_1$) of the cold and hot temperature contacts of the rectangular sample.

The Seebeck coefficient, S is thus calculated by:

$$S= (-V_{th})/(T_{hot}- T_{cold}) \quad (1)$$

(Linseis Messgeräte GmbH, 2023)

$$S= (-V_{th})/(T_2- T_1) \quad (2)$$

(Linseis Messgeräte GmbH, 2023)

Where,

V_{th} is the Seebeck voltage generated by the temperature difference across the material.

To determine the specific electric resistance (or the electrical conductivity) of the sample, the four-terminal DC measurement technique was employed. The influences in contact or wire resistance were suppressed to significantly enhance the measurement accuracy.

Under thermal equilibrium conditions for measurement ($\Delta T = 0$), a one-dimensional constant current flow was impressed into the sample. The resulting voltage drop, V over a portion of length L of the sample is again measured using one of the thermocouple wires.

The electrical conductivity, ϱ can be calculated by:

$$\rho= V/I \cdot A/L \quad (3)$$

(Linseis Messgeräte GmbH, 2023)

Where,

I is the magnitude of current flow, and

A is the cross-sectional area of the sample.

The Harman method allows the calculation of the thermoelectric figure of merit, ZT of a material from the measurement of the temporal voltage curve of the sample with applied direct current. The impressed current into the thermoelectric sample was measured via two needle contacts based on the Peltier effect. One of the two transitions was locally heated or cooled as a result of the temperature difference established over the sample due to the adiabatic boundary conditions.

The dimensionless figure of merit, ZT can be calculated from:

$$ZT= V_{th}/V_{\Omega} \quad (4)$$

(Linseis Messgeräte GmbH, 2023)

Where,

V_{Ω} is the voltage due to the impressed current, I.

The thermal conductivity, k is given as:

$$k= (L/A) ((V_{th}-IR)/(T_2- T_1)) \quad (5)$$

(Linseis Messgeräte GmbH, 2023)

Where,

R is the electrical resistance of the sample.

Simulation of Synthesized TEPG Material

The simulation of the synthesized TEPG material was done using ANSYS Workbench Thermal-Electric modules. The simulation involved several detailed steps, from model preparation to result analysis. First, a 3D geometry of the thermoelectric module was created with the help of the DesignModeler in ANSYS. Then, input engineering data parameters from experimental results as shown in Table 1, were created as material properties. Afterwards meshing was done to smoothen small areas such as the electrodes. The electrodes used were Copper (Cu) and Al_2O_3 (Ceramics) for the hot side and cold side respectively (Pramudi *et al.*, 2024; Harsito *et al.*, 2022b). For meshing, the element type used was Heaedral with mesh sizes of 0.1mm, 0.05mm, and 0.01mm used on the sides of the thermoelectric, ceramics, and copper legs respectively. The convergence criterion was set to when the residuals fall below 10e-5. For solver settings, Steady-State Thermal-Electric Conduction, relative tolerance: 10e-5, and maximum iterations: 1000, were used. The boundary conditions of the simulation such as heat sources, cold areas, material properties from all dimensions, as well as connection barriers (RL) or external barriers, are shown in Figure 1 below. Finally, the simulations were run

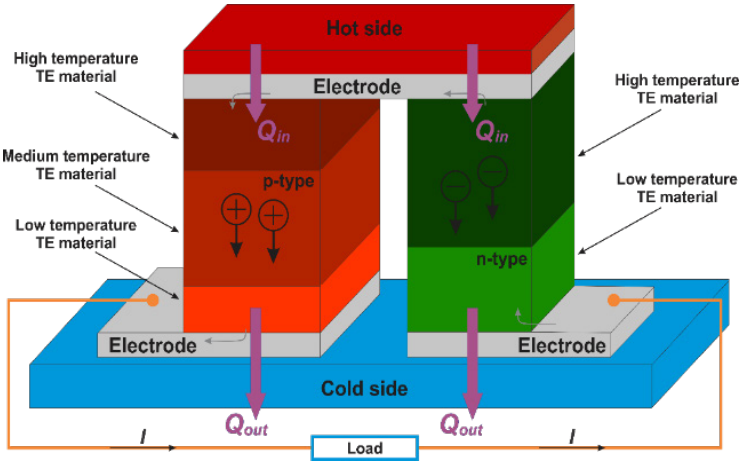

Figure 1: Boundary conditions of simulated TEPG material model

under a computational time of 12:03:54, followed by post-processing and analysis of results.

The best p-type TE materials were chosen for the compatibility study, from Bi_2Te_3 alloy for room temperature, to $CeFe_4Sb_{12}$ for mid-temperature, and to PbTeS and Zn_2Sb_3 application. On the other hand, three distinctive n-type material combinations are used for comparison and conclusion without loss of generality.

RESULTS AND DISCUSSION

Experimental/Simulation Result

Table 1: Simulated TEPG material properties versus figures of merit

Synthesized TE Material	Compatibility Materials	Material Type	Temperature Distribution [K]	Electrical Resistivity [Ω.m]	Thermal Conductivity [$Wm^{-1}K^{-1}$]	Figure of Merit [ZT]
BixSbyTez (Vikhor & Anatychuk, 2009)	Bi_2SbTe_3	Leg+	300 – 400	2.8×10^{-8}	6.30×10^{-7}	1.40
BixTez (Sudharshan *et al.*, 2016)	Bi_2Te_3	Leg+	350 – 500	3.9×10^{-7}	5.96×10^{-7}	1.43
ZnxSby (Moreno *et al.*, 2018)	Zn_2Sb_3	Leg+	450 – 550	1.3×10^{-6}	5.80×10^{-7}	1.44
CeFewSb$_{12}$ (Zaman *et al.*, 2017)	$CeFe_4Sb_{12}$	Leg- 3	600 – 650	6×10^{-8}	4.10×10^{-7}	1.45
Te/Ag/Ge/Sb Alloys (Fraisse *et al.*, 2013)	Te/Ag/Ge/Sb	Leg- 3	600 – 800	5.6×10^{-8}	3.50×10^{-7}	1.50
CexFeyCozSb$_{12}$ (Muthu *et al.*, 2019)	$Ce_{0.5}Fe_{3.5}Co_{0.5}Sb_{12}$	Leg- 1	800 – 1000	1.7×10^{-8}	2.98×10^{-7}	1.56
ScxCoySbz (Du & Wen, 2011)	ScCoSb	Leg- 2	850 – 1000	1.3×10^{-7}	2.43×10^{-7}	1.61
MoxSbyTez (He *et al.*, 2019)	$Mo_3Sb_4Te_{1.6}$	Leg- 2	1000 – 1150	4.6×10^{-1}	1.7×10^{-7}	1.58
SiGe (Maduabuchi *et al.*, 2021)	SiGe	Leg- 1	1100 – 1250	6.4×10^{-2}	1.69×10^{-7}	1.60

Results from SEM

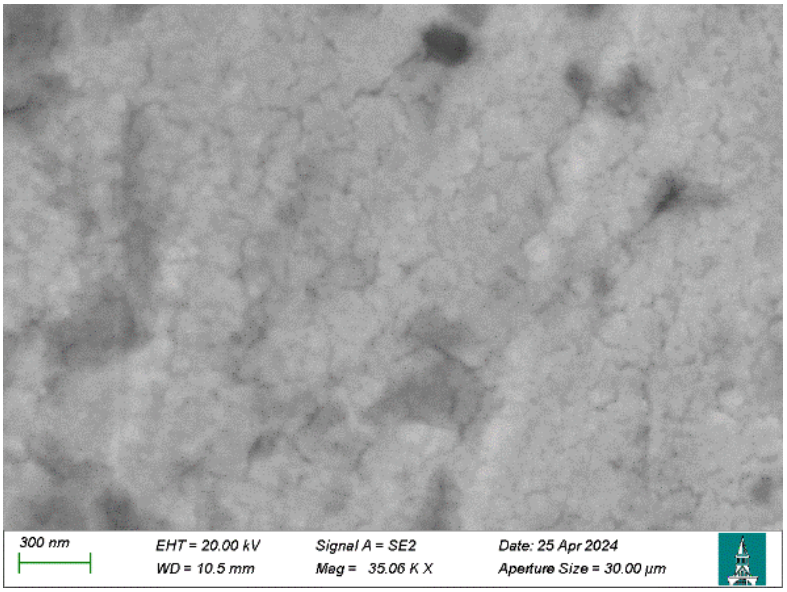

Figure 2: Morphology under constant deposition

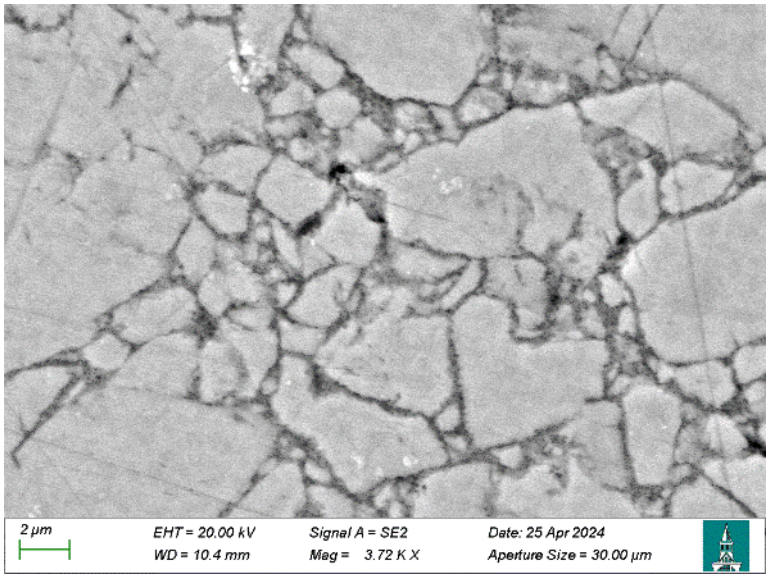

Figure 3: Morphology under controlled pulsed deposition

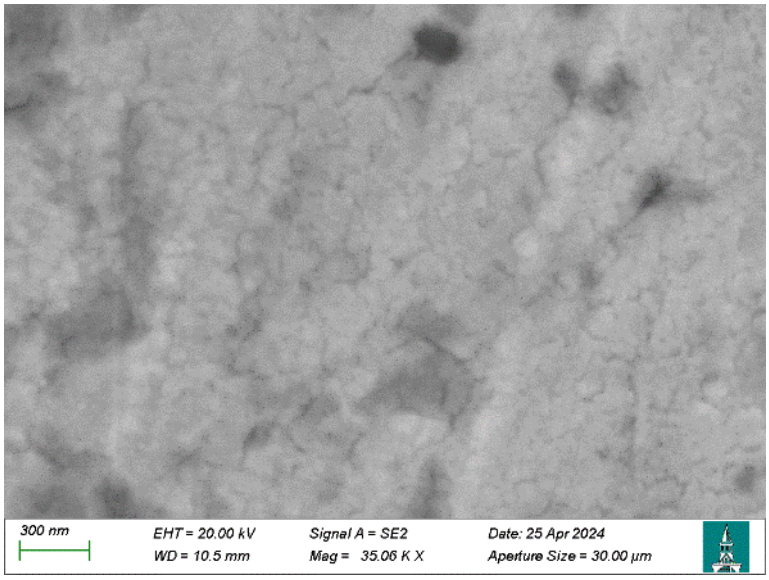

Figure 4: Cross-sectional SEM image

Figures 2 and 3 show the deposition-synthesized materials under constant and pulsed deposition conditions respectively. The constant deposited film (Figure 2) exhibits an initial 6U-thick compact layer as the main layer, while the top includes pillar structure layers. Though a thicker film of the synthesized thermoelectric material can be achieved by further deposition, its mechanical strength will be very weak due to its porous layer structure. The thick electrodeposited film by the constant condition is easily peeled off for the substrate layer. To overcome this problem, pulsed deposition has been conducted. Compared with the constant electrochemical deposition, the pulsed electrodeposition with a pulse delay time for the recovery of the ion concentration always leads to a crystalline structure with high orientation and good uniformity. This is proven in Figure 3. The deposited surface under pulsed conditions is more uniform and smoother than that under constant conditions. Figure 4 shows a representative cross-sectional SEM image of the 300 µm-thick $HoSb_xTe_x$ deposition film, which is comparable to the bulk $HoSb_xTe_x$ material.

Profile Temperature

Figures 5 - 12 below show the temperature distribution of different leg materials of Leg- 1, Leg- 2, and Leg-3 from 300K up to 1000K. This result stems from combining the current selected synthesized Leg+ materials Bi_2SbTe_3, Zn_2AgSb_3, PbTeS, SnSe with the strongest synthesized Leg- materials, Cu-Doped BiTeSe, AgPbSb, and SiGe.

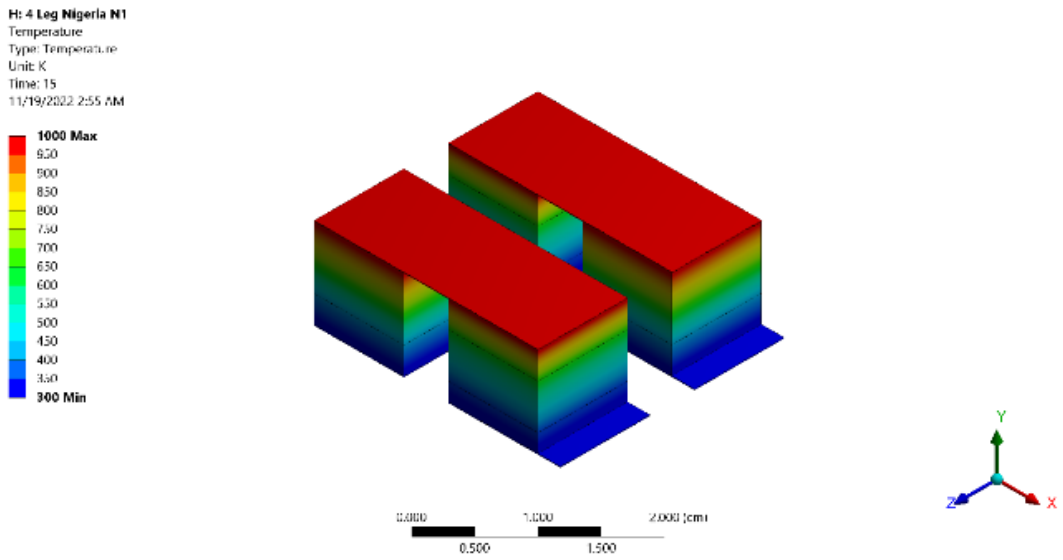

Figure 5: Temperature distribution on 4 Leg -1 material

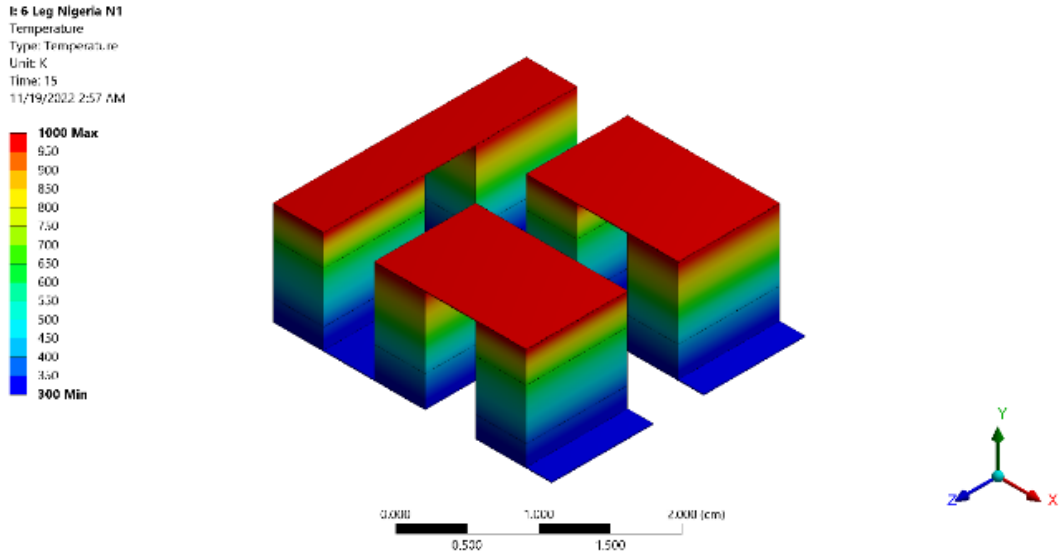

Figure 6: Temperature distribution on 6 Leg -1 material

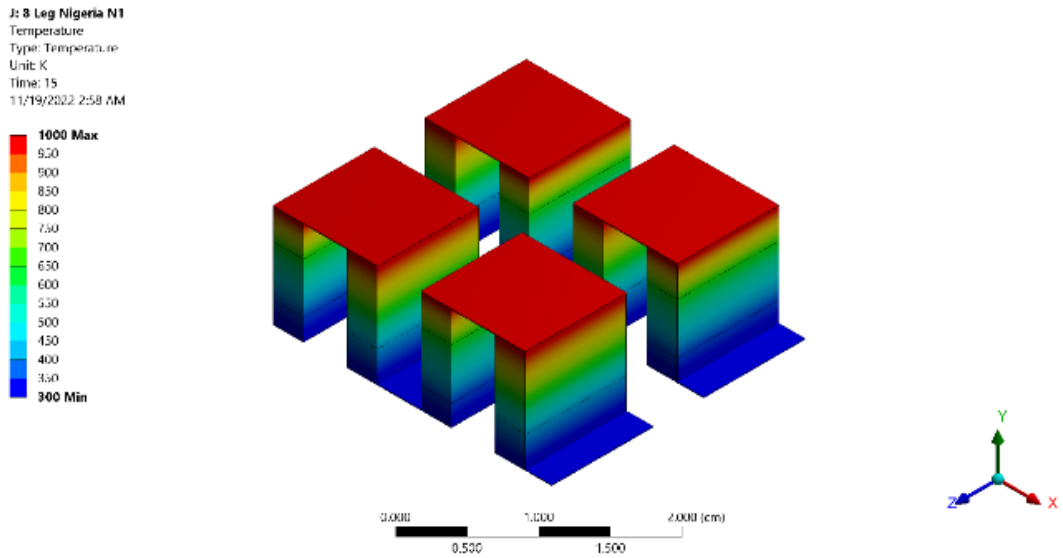

Figure 7: Temperature distribution on 8 Leg -1 material

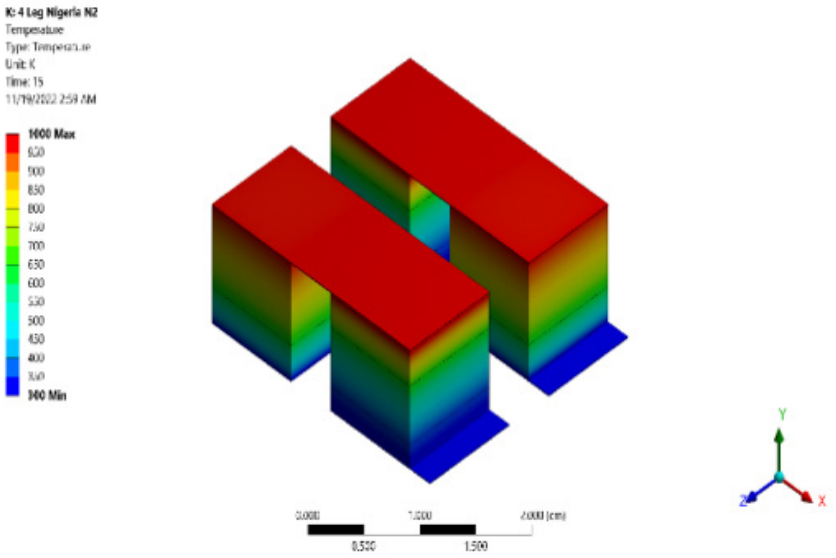

Figure 8: Temperature distribution on 4 Leg -2 material

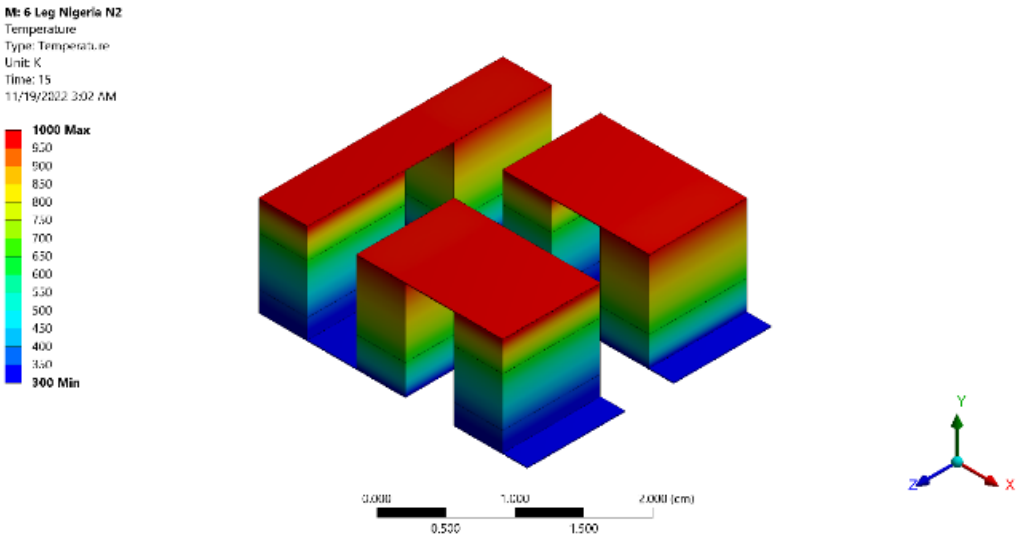

Figure 9: Temperature distribution on 6 Leg -2 material

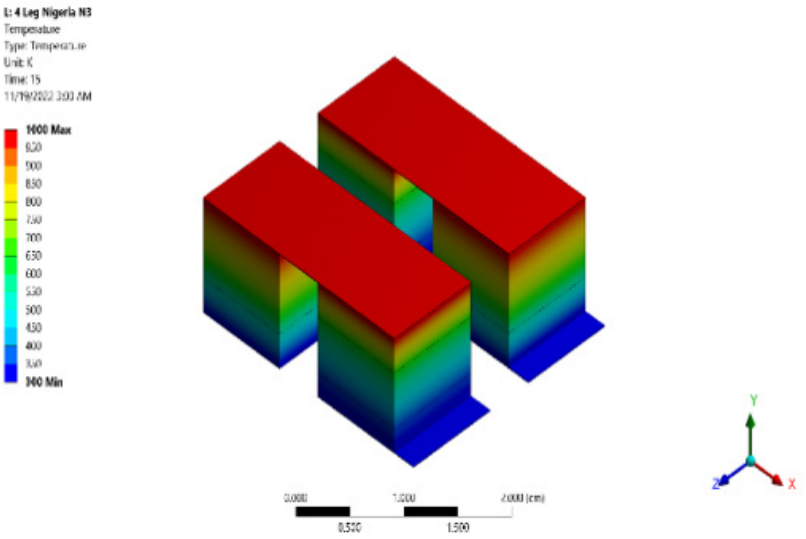

Figure 10: Temperature distribution on 4 Leg -3 material

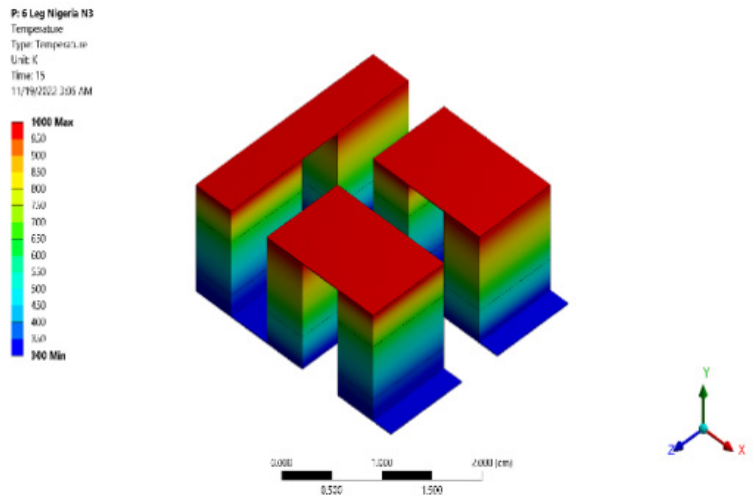

Figure 11: Temperature distribution on 6 Leg -3 material

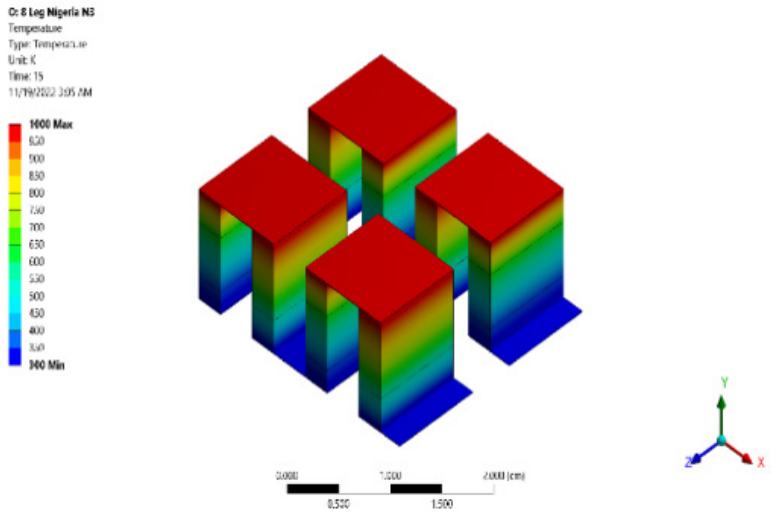

Figure 12: Temperature distribution on 8 Leg -3 material

A careful consideration of the thickness and uniformity of the colored patches in Figures 5 - 12, shows that Leg-1 materials are more compatible for thermal transport in thermoelectric power generation based on temperature distribution across the selected material.

Thermoelectric Generation Efficiency Based on Total Number of Legs

Figure 13 shows the plot of TEPG efficiency against the number of legs of the thermoelectric material.

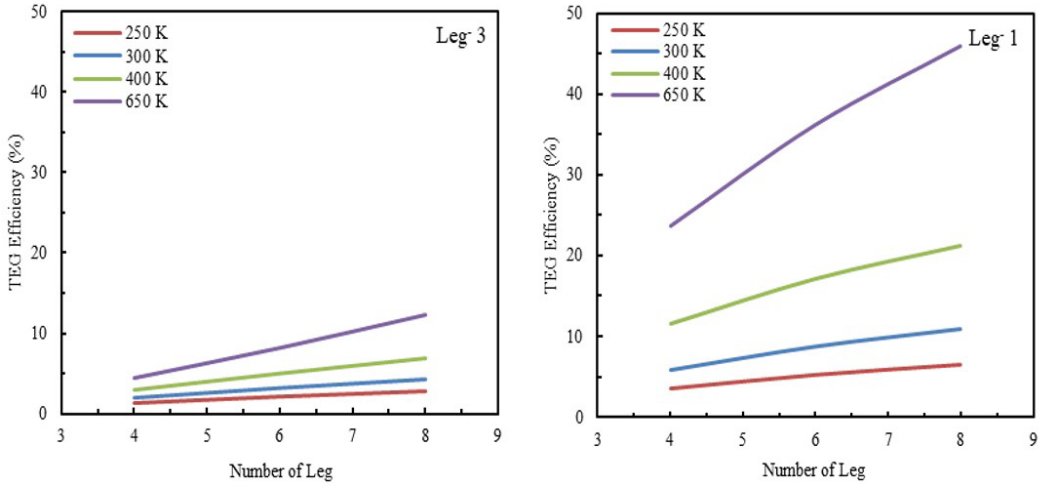

Figure 13: Plot of TEG efficiency versus number of legs

From the plots above, the increase in the number of legs as well as in the operating temperature, leads to a relative increase in TEG efficiency. The Leg-1 type materials show a sharper response to changes in this regard, hence they are considered superior based on efficiency as a result of the number of material legs.

Thermoelectric Generation Configuration

Figure 14 shows the TE generation configuration. This was determined by plotting output voltage (V) versus number of Legs, heat absorbed power (W) versus temperature differences (K), and heat flux (W/mm2) versus temperature differences (K).

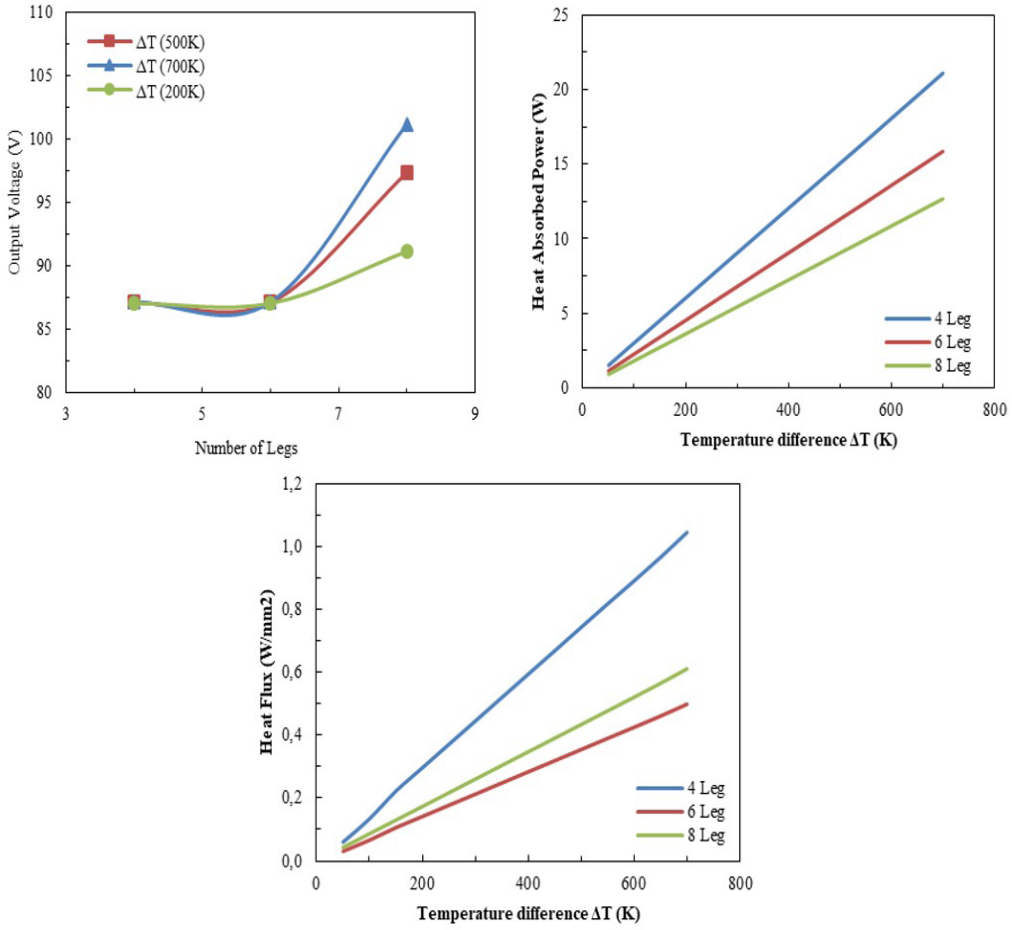

Figure 14: TEPG configuration

The plot of output voltage versus temperature difference shows that the output voltage of TEPGs can significantly be increased by the number of legs. Also, since both the heat absorbed power and heat flux are directly proportional to thermal conductivity, the plots of the heat absorbed power and heat flux against temperature difference therefore show that an increase in the number of legs leads to a decrease in thermal conductivity, and by extension an increase in the efficiency of TEPGs.

Heat Absorbed on 2, 3 and 4 Leg Pairs

Figure 15 shows the plots of heat absorbed (W) versus

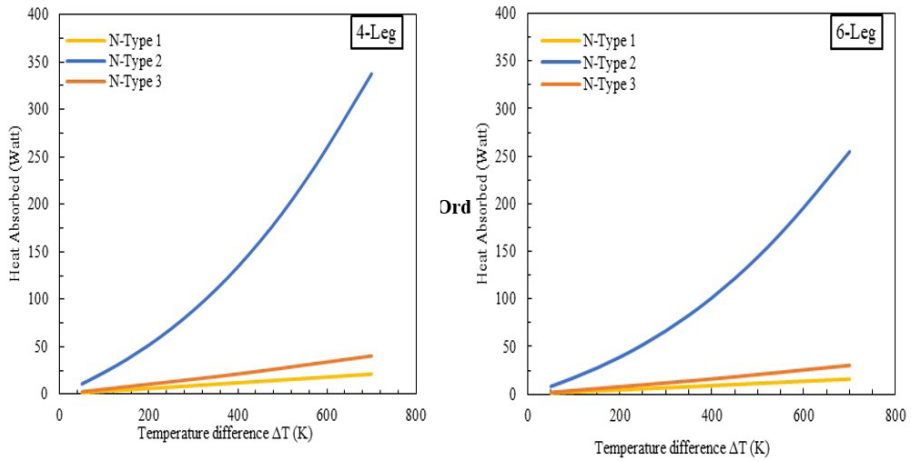

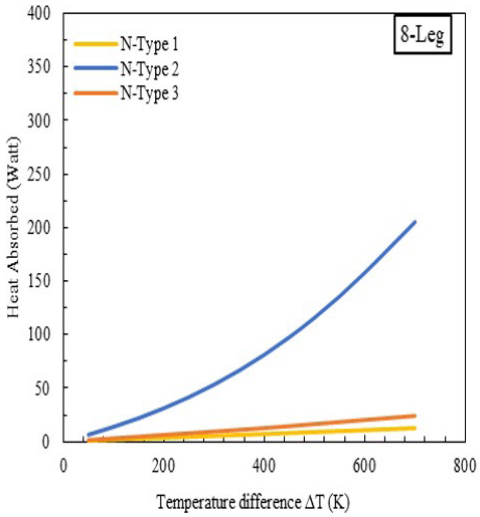

Figure 15: Heat Absorbed on 2, 3, and 4 Leg pairs

temperature difference for 2, 3, and 4 leg pairs of thermoelectric generators from different Leg- materials.

From the figure, and in conjunction with the observation from Figures 13 and 14, N-Type 1 materials are more suitable for thermoelectric power generation, since they have lower heat absorption power, leading to lower thermal conductivity which is desirable for thermal transport.

TEG Efficiency Based on High Temperatures

Figure 16 shows TEPG efficiency based on high temperatures, (a) 2 pairs (4-Leg), (b) 3 pairs (6-Leg), and (c) 4 pairs (8-Leg).

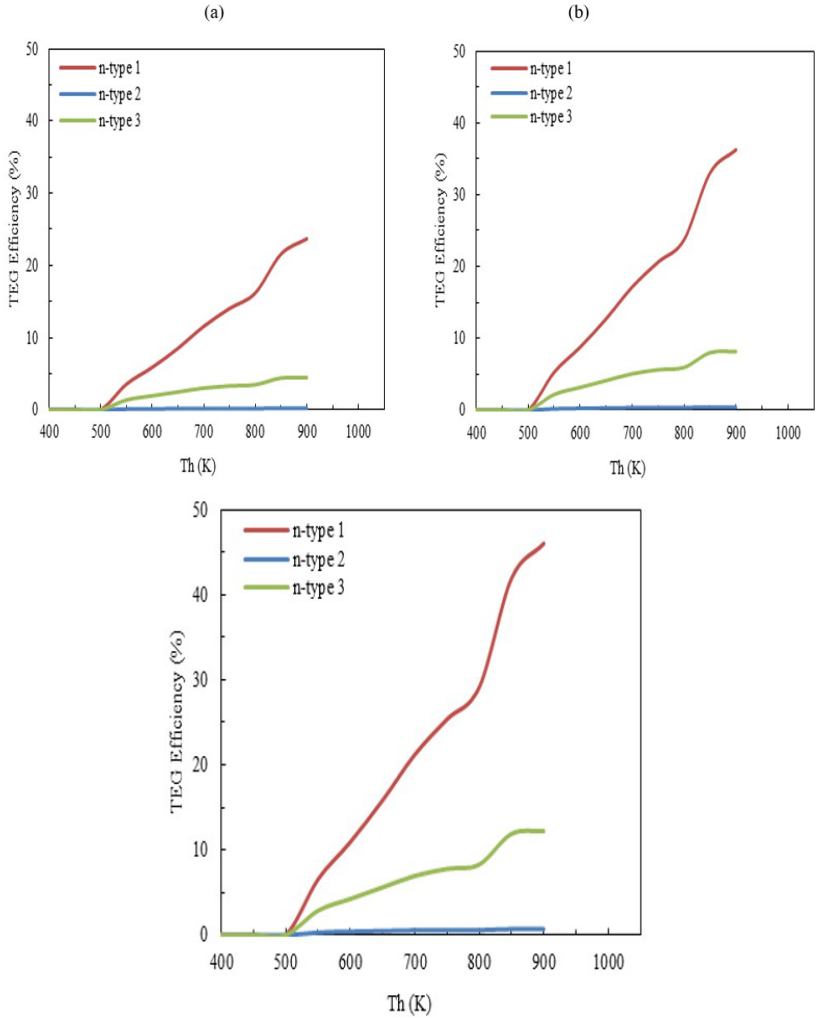

Figure 16: TEPG efficiency based on hot temperature, (a) 2 pairs (4-Leg), (b) 3 pairs (6-Leg), (c) 4 pairs (8-Leg)

From the figure, n-type 1 materials have superior TEG efficiency over a broad range of temperatures, thus making them ideal for high-temperature thermoelectric applications. The figure also shows that an increase in the number of legs causes a relative increase in overall TEPG efficiency.

Quantitative Comparison of Results with Prior Studies

Zheng *et al.* optimized the thermoelectric properties of SiGe based on function-matching nanoparticles. TaC was incorporated as a composite into SiGe alloys via mechanical alloying and spark plasma sintering. A peak ZT value of the bulk composite was attained at 873K to be 1.06. However, in this study, the deposition of HoSbxTex on SiGe gave rise to a ZT value of 1.6 at an operating temperature range of 1100K – 1250K.

Similarly, Morozkin & Nikiforov studied the thermoelectric properties of ScCoSb and obtained a peak ZT value of 0.009 at 380K. However, in this study, a ZT value of 1.61 was obtained at a temperature range of 850K – 1000K.

These studies in relation, show that the thermoelectric figure of merit and overall efficiency of TE materials can be significantly enhanced through an increase in temperature, material compositions, synthesis routes, and device architectures.

Influence of Microstructure, Composition & Interfaces on Transport Properties

The microstructure of synthesized materials can significantly influence the thermal and electrical transport properties of synthesized materials. Smaller grain sizes (at grain boundaries), nanostructures (e.g., nanowires), as well as defects and dislocations (that act as phonon scattering centers) can enhance phonon scattering, thus lowering thermal conductivity. However, optimal grain boundary engineering, proper nanostructure designs, and controlled introduction of defects must be taken into consideration to ensure that the decrease in thermal conductivity does not severely impact, but rather improves overall electrical performance.

Also, the elemental composition of synthesized materials as well as alloying and doping can influence transport properties. Phonon dynamics is impacted by the choice of elements and their respective masses, as heavy atoms typically have lower phonon frequencies, thereby lowering thermal conductivity. Incorporating elements that provide additional charge carriers can also enhance electrical conductivity. Alloying and doping help to introduce mass fluctuations and strain field scattering, hence reducing thermal conductivity. Doping can also be used to control charge carrier concentration and significantly impact electrical conductivity, as n-type doping increases electron concentration while p-type doping increases hole concentration.

Similarly, interfaces of synthesized materials such as grain boundaries with respect to boundary density and structure, contribute to phonon scattering, thus lowering thermal conductivity. However, since grain boundaries can impede carrier mobility thus reducing electrical conductivity, it is pertinent to design smooth, low-resistance boundaries to mitigate this effect.

Analysis of Discrepancies or Unexpected Results

The compatibility factor of a material may deviate from the ideal range owing to several reasons including inhomogeneous doping, poor grain boundary quality, thermal instability, and defect density among others. Advanced doping techniques like ion implantation or co-precipitation can be used to mitigate inhomogeneous doping and achieve a more uniform dopant distribution. Techniques like spark plasma sintering and hot pressing can be employed to reduce resistance and improve grain boundary quality. To counter thermal instability, materials with stable phases over the operating temperature range should be selected. Protective coatings can also be introduced to prevent oxidation. On the other hand, post-synthesis annealing under controlled atmospheres as used in this study, can help reduce defect density and improve material properties.

Areas for Further Exploration

Some key areas for further exploration to improve the performance and compatibility of TEPG materials include; developing composite materials that combine desired properties of constituent materials, optimizing leg geometry through advanced investigation of the impact of aspect ratio (length to cross-sectional area), and different leg shapes, exploring high-temperature materials whilst improving thermal management techniques, assessing the performance and lifecycle of materials under varying economic (cost, abundance, non-toxicity, etc.) and environmental (pressure variations, moisture, mechanical vibrations, UV exposure, chemical exposure etc.) conditions, to mention but a few.

Specifically, future research directions aimed at potentially overcoming the current limitations in the transport properties of synthesized materials and achieving high performance should include improving material compositions through the use of high-entropy alloys that consist of five or more elements in near-equiatomic ratios (e.g., CoCrFeMnNi, AlCoCrFeNi, AlCoCrFeMoNi, FeCoNiCuCr, etc.), as they show significant lattice distortion, phonon scattering, and offer adequate compositional space for tailoring their transport properties. Nanocomposites like Bi_2Te_3 with nano-inclusions of carbon or silicon can also be incorporated to effectively scatter phonons and improve transport properties. Furthermore, complex chalcogenides such as tetrahedrites and skutterudites can be introduced to create intrinsic phonon scattering sites to effectively reduce thermal conductivity.

Synthesis routes like mechanical alloying via ball milling and hot pressing should be employed to design materials with refined grain sizes and uniform distribution of dopants. Chemical vapor deposition can also be incorporated

to synthesize layered heterostructured materials with tailored properties. Similarly, spark plasma sintering can be used to produce high-density materials with minimal grain growth, thereby preserving nanostructures capable of scattering phonons.

Device architectures like nanostructured thin films (thin films with embedded nanostructures like SiGe thin films with embedded Ge nanodots, Bi_2Te_3 thin films with embedded Sb_2Te_3 quantum dots, PbTe thin films with PbSe nano-inclusions, TiO_2 thin films with Au particles, etc.) can be employed to achieve high performance, as the embedded nanostructures help to scatter phonons and reduce thermal conductivity with the thin film structure facilitating efficient electron transport. Superlattice structures consisting of alternating layers of different materials at the nanoscale (e.g., Bi_2Te_3/ Sb_2Te_3 superlattices) can also significantly enhance phonon scattering, allow electron transport, reduce thermal conductivity, leading to improved thermoelectric efficiency.

CONCLUSION

The findings of this research paper are summarized below.

• Tailored material design is crucial to achieving synergistic enhancements in both thermal and electrical conductivity, thereby advancing the efficiency and viability of thermoelectric energy conversion technologies.

• An increase in the number of legs as well as in the operating temperature, leads to a relative increase in output voltage and TEG efficiency.

• N-type 1 materials have superior TEG efficiency over a broad range of temperatures, thus making them ideal for high-temperature thermoelectric applications.

• ZT values in the range of 1.5 – 1.6 can be achieved for synthesized materials under high-temperature conditions.

REFERENCES

Ali, H., Yilbas, B. S., & Al-Sharafi, A. (2018). Segmented thermoelectric generator: exponential area variation in leg. *International Journal of Energy Research, 42*(2), 477–489. https://doi.org/https://doi.org/10.1002/er.3825

Du, C. Y., & Wen, C. Da. (2011). Experimental investigation and numerical analysis for one-stage thermoelectric cooler considering Thomson effect. *International Journal of Heat and Mass Transfer, 54*(23–24), 4875–4884. https://doi.org/10.1016/J.IJHEATMASSTRANSFER.2011.06.043

Ferreira-Teixeira, S., & Pereira, A. M. (2018). Geometrical optimization of a thermoelectric device: Numerical simulations. *Energy Conversion and Management, 169,* 217–227. https://doi.org/10.1016/J.ENCONMAN.2018.05.030

Fraisse, G., Ramousse, J., Sgorlon, D., & Goupil, C. (2013). Comparison of different modeling approaches for thermoelectric elements. *Energy Conversion and Management, 65,* 351–356. https://doi.org/10.1016/J.ENCONMAN.2012.08.022

Harsito, C., Purba, D. A., Mufti Reza Aulia, P., Triyono, T., & Permata, A. N. S. (2022). Mini Review of Thermoelectric Application with LFP 18650 Battery in Forest Exploration Campfire. *AIP Conference Proceedings, 2499*. https://doi.org/10.1063/5.0104938

Harsito, C., Reza, M., Putra, A., & Purba, D. A. (n.d.). *Mini review of thermoelectric and their potential applications in vehicles.*

Harsito, C., Triyono, T., & Rovianto, E. (2022a). Analysis of Heat Potential in Solar Panels for Thermoelectric Generators using ANSYS Software. *Civil Engineering Journal (Iran), 8*(7), 1328–1338. https://doi.org/10.28991/CEJ-2022-08-07-02

He, H., Liu, W., Wu, Y., Rong, M., Zhao, P., & Tang, X. (2019). An approximate and efficient characterization method for temperature-dependent parameters of thermoelectric modules. *Energy Conversion and Management, 180,* 584–597. https://doi.org/10.1016/J.ENCONMAN.2018.11.002

Karthick, K., Suresh, S., Joy, G. C., & Dhanuskodi, R. (2019). Experimental investigation of solar reversible power generation in thermoelectric generator (TEG) using thermal energy storage. *Energy for Sustainable Development, 48,* 107–114. https://doi.org/10.1016/J.ESD.2018.11.002

Lee, M.-Y., Seo, J.-H., Lee, H.-S., & Garud, K. S. (2020). Power generation, efficiency, and thermal stress of thermoelectric module with leg geometry, material, segmentation, and two-stage arrangement. *Symmetry, 12*(5), Article 786. https://doi.org/10.3390/sym12050786

Linseis Messgeräte GmbH. (2023, July). *LSR-3 Seebeck-coefficient/resistivity/Harman-method/ZT of modules.* Linseis. https://www.linseis.com/en/products/thermoelectric/lsr-3/

Ma, X., Shu, G., Tian, H., Xu, W., & Chen, T. (2019). Performance assessment of engine exhaust-based segmented thermoelectric generators by length ratio optimization. *Applied Energy, 248,* 614–625. https://doi.org/10.1016/J.APENERGY.2019.04.103

Maduabuchi, C. C., & Mgbemene, C. A. (2020). Numerical Study of a Phase Change Material Integrated Solar Thermoelectric Generator. *Journal of Electronic Materials, 49*(10), 5917–5936. https://doi.org/10.1007/s11664-020-08331-3

Maduabuchi, C., Ejenakevwe, K., Ndukwe, A., & Mgbemene, C. (2021). High performance solar thermoelectric generator using asymmetrical variable leg geometries. *E3S Web of Conferences, 239,* Article 00005. https://doi.org/10.1051/e3sconf/202123900005

Maduabuchi, C., & Gurevich, Y. (2021). Theoretical investigation on the influence of Seebeck and Thomson effects in a thermoelectric generator. *Research Square.* https://doi.org/10.21203/rs.3.rs-421044/v1

Moreno, R., Pollman, A., & Grbovic, D. (2018). Harvesting waste thermal energy from military systems. *ASME Power Conference.* https://doi.org/10.1115/POWER2018-7514

Morgan K. A., Tang T., Zeimpekis I., Ravagli A., Craig C., Yao J., Feng Z., Yarmolich D., Barker C., Assender H., Hewak D. W. (2019). High-throughput physical vapour deposition flexible thermoelectric generators. *Scientific Reports, 9,* 4393. https://doi.org/10.1038/s41598-019-41000-y

Morozkin A.V. & Nikiforov, V.N. (2005). Thermoelectric Properties of ScCoSb, ScNi0.86Sb,, and MgNiSb Compounds. *Journal of Alloys and Compounds, 400,* 62 - 66. https://doi.org/10.1016/j.jallcom.2005.04.012

Muthu, G., Shanmugam, S., & Veerappan, A. R. (2019). Theoretical and Experimental Study on a Thermoelectric Generator Using Concentrated Solar Thermal Energy. *Journal of Electronic Materials, 48*(5), 2876–2885. https://doi.org/10.1007/s11664-019-07024-w

Olivares-Robles, M. A., Badillo-Ruiz, C. A., & Ruiz-Ortega, P. E. (2020). A comprehensive analysis on nanostructured materials in a thermoelectric micro-system based on geometric shape, segmentation structure, and load resistance. *Scientific Reports, 10*(1), 21659. https://doi.org/10.1038/s41598-020-78770-9

Pallavi, B., Sawanta, S., Kishorkumar, V., Vijay, V., Vishvanath, B., Rahul, M., Rohini, R., & Popatrao, N. (2016). Synthesis of Bismuth Telluride Thin Film for Thermoelectric Application Via Electrodeposition Technique. *Macromol. Symp., 361,* 152-155. https://doi.org/10.1002/masy.201400234

Pramudi, G., Harsito, C., Muslim, R., & Adika, D. (2024). Investigation of a thermoelectric generator with sandwich leg modification. *International Journal of Engineering and Applied Sciences, 12,* 87–93. https://doi.org/10.15866/irea.v12i2.23648

Qiu, C., & Shi, W. (2020). Comprehensive modeling for optimized design of a thermoelectric cooler with non-constant cross-section: Theoretical considerations. *Applied Thermal Engineering, 176,* 115384. https://doi.org/10.1016/J.APPLTHERMALENG.2020.115384

Shittu, S., Li, G., Zhao, X., & Ma, X. (2020). Review of thermoelectric geometry and structure optimization for performance enhancement. *Applied Energy, 268,* 115075. https://doi.org/10.1016/J.APENERGY.2020.115075

Sudharshan, K. Y., Kumar, V. P., & Barshilia, H. C. (2016). Performance evaluation of a thermally concentrated solar thermo-electric generator without optical concentration. *Solar Energy Materials and Solar Cells, 157,* 93–100. https://doi.org/10.1016/J.SOLMAT.2016.05.033

Thimont, Y., & LeBlanc, S. (2019). The impact of thermoelectric leg geometries on thermal resistance and power output. *Journal of Applied Physics, 126*(9), 95101. https://doi.org/10.1063/1.5115044

Twaha S., Zhu J., Yan Y., Li B. (2016). A comprehensive review of thermoelectric technology: Materials, applications, modelling and performance improvement. *Renewable and Sustainable Energy Reviews, 65,* 698-726. https://doi.org/10.1016/j.rser.2016.07.034

Vikhor, L. N., & Anatychuk, L. I. (2009). Generator modules of segmented thermoelements. *Energy Conversion and Management, 50*(9), 2366–2372. https://doi.org/10.1016/J.ENCONMAN.2009.05.020

Wang, R., Meng, Z., Luo, D., Yu, W., & Zhou, W. (2020). A Comprehensive Study on X-Type Thermoelectric Generator Modules. *Journal of Electronic Materials, 49*(7), 4343–4354. https://doi.org/10.1007/s11664-020-08152-4

Wang, X. D., Huang, Y. X., Cheng, C. H., Ta-Wei Lin, D., & Kang, C. H. (2012). A three-dimensional numerical modeling of thermoelectric device with consideration of coupling of temperature field and electric potential field. *Energy, 47*(1), 488–497. https://doi.org/10.1016/J.ENERGY.2012.09.019

Wu, S.Y., Zhang, Y.-C., & Xiao, L. (2018). Conceptual design and performance analysis of concentrated solar-driven TIC/AMTEC/TEG hybrid system. *International Journal of Energy Research, 42*(15), 4674–4686. https://doi.org/https://doi.org/10.1002/er.4209

Wu, Y., Yang, J., Chen, S., & Zuo, L. (2018). Thermo-element geometry optimization for high thermoelectric efficiency. *Energy, 147,* 672–680. https://doi.org/10.1016/J.ENERGY.2018.01.104

Xiao F., Hangarter C., Yoo B., Rheem Y., Lee K., Myung N. V. (2008). Recent progress in electrodeposition of thermoelectric thin films and nanostructures. *Electrochimica Acta,, 53,* 8103-8117. https://doi.org/10.1016/j.electacta.2008.06.015

Yoo I., Myung N. V., Lim D. C., Song Y., Jeong Y., Kim Y. D., Lee K. H., Lim J. (2013). Electrodeposition of BixTey thin films for thermoelectric application. *Thin Solid Films, 546,* 48-52. https://dx.doi.org/10.1016/j.tsf.2013.05.036

Zaman, H. U., Shourov, C. E., Mahmood, A. Al, & Siddique, N. E. A. (2017). Conversion of wasted heat energy into electrical energy using TEG. In *2017 IEEE 7th Annual Computing and Communication Workshop and Conference (CCWC)* (pp. 1–5). https://doi.org/10.1109/CCWC.2017.7868452

Zhang, A. B., Wang, B. L., Pang, D. D., Chen, J. B., Wang, J., & Du, J. K. (2018). Influence of leg geometry configuration and contact resistance on the performance of annular thermoelectric generators. *Energy Conversion and Management, 166,* 337–342. https://doi.org/10.1016/J.ENCONMAN.2018.04.042

Zheng, F., Jisheng, L., Jun-Liang, C., Ying, P., Huajun, L., Jian, N., Chengyan, L., Wangyang, D., & Lei, M. (2023). Realizing high thermoelectric performance for p-type SiGe in the medium temperature region via TaC compositing. *Journal of Materiomics.* https://doi.org/10.1016/j.jmat.2023.03.004

Zhu, L., Li, H., Chen, S., Tian, X., Kang, X., Jiang, X., & Qiu, S. (2020). Optimization analysis of a segmented thermoelectric generator based on genetic algorithm. *Renewable Energy, 156,* 710–718. https://doi.org/10.1016/J.RENENE.2020.04.120